GA–A27416

EXPERIMENTAL TESTS OF STIFFNESS IN THE ELECTRON AND ION ENERGY TRANSPORT IN THE DIII-D TOKAMAK

by

T.C. LUCE, C. HOLLAND, S.P. SMITH, K.H. BURRELL, J.C. DeBOO, J.E. KINSEY, A. MARINONI, P. MANTICA, M.E. AUSTIN, E.J. DOYLE, C.C. PETTY, and L. ZENG

OCTOBER 2012

GENERAL ATOMICS

DISCLAIMER

GA–A27416

EXPERIMENTAL TESTS OF STIFFNESS IN THE ELECTRON AND ION ENERGY TRANSPORT IN THE DIII-D TOKAMAK

by
T.C. LUCE, C. HOLLAND,* S.P. SMITH, K.H. BURRELL, J.C. DeBOO, J.E. KINSEY, A. MARINONI,† P. MANTICA,‡ M.E. AUSTIN,# E.J. DOYLE,¶ C.C. PETTY, and L. ZENG¶

This is a preprint of a paper to be presented at the Twenty-fourth IAEA Fusion Energy Conf., October 8-13, 2012 in San Diego, California.

*University of California San Diego, La Jolla, California.
†Massachusetts Institute of Technology, Cambridge, Massachusetts.
‡Associazione Euratom-ENEA-CNR, Milano, Italy.
#University of Texas at Austin, Austin, Texas.
¶University of California Los Angeles, Los Angeles, California.

Work supported in part by
the U.S. Department of Energy
under DE-FC02-04ER54698, DE-FG02-07ER54917, DE-FG02-94ER54235,
DE-FG03-97ER54415, and DE-FG02-08ER54984

GENERAL ATOMICS PROJECT 30200
OCTOBER 2012

GENERAL ATOMICS

Experimental Tests of Stiffness in the Electron and Ion Energy Transport in the DIII-D Tokamak

T.C. Luce 1), C. Holland 2), C.C. Petty 1), S.P. Smith 1), K.H. Burrell 1), J.C. DeBoo 1), J.E. Kinsey 1), A. Marinoni 3), M.E. Austin 4), E.J. Doyle 5), and L. Zeng 5)

1) General Atomics, San Diego, California 92186-5608, USA
2) University of California San Diego, 9500 Gilman Dr., La Jolla, California 92093-0417, USA
3) Massachusetts Institute of Technology, 77 Massachusetts Ave., Cambridge, Massachusetts 02139, USA
4) University of Texas at Austin, 2100 San Jacinto Blvd, Austin, Texas 78712-1047, USA
5) University of California Los Angeles, PO Box 957099, Los Angeles, California 90095-7099, USA

E-mail: luce @fusion.gat.com

Abstract. Experiments to test the hypothesis of strong transport beyond a critical gradient threshold are presented. In L mode, electron cyclotron heating was used to make local modifications to the electron temperature gradient, while leaving other quantities relatively unchanged. Clear evidence is seen for both a threshold in gradient and strong transport beyond this threshold. In H mode, scans of neutral beam injection power at two levels of torque were used to look for an influence of $E_r x B$ shear, in addition to looking for threshold behavior. No evidence of strong transport limiting the increase of the ion temperature gradient is found, with the possible exception of the low torque case near ρ=0.7. Circumstantial evidence for a threshold is found, but the threshold level lies at or below the level of power flow needed to maintain the H mode.

1. Introduction

For many years it has been noted that measured electron and ion temperature profile shapes have remarkably little variation with heating power and location in tokamaks [1]. This has been attributed to many different causes, including global constraints minimizing the free energy [2], connection between the current density and electron temperature profiles beyond neoclassical theory [3], global entropy production [4], or the existence of non-diffusive transport mechanisms [5]. But the most enduring picture invokes the onset of turbulence (usually due to unstable electrostatic drift waves) beyond a threshold in the electron or ion temperature gradient that supplies the free energy for the instability [6]. In this picture, the release of free energy is so strong that the gradient needs to increase hardly at all to exhaust large increments in the power flowing through that location in the plasma. The result of this virulent instability on the electron or ion temperature profile would then be to render it insensitive to additional heating power deposited in the center of the plasma. This is referred to colloquially as "stiffness". The purpose of the experiments reported here is to examine the behavior of the electron and ion temperature profiles in L-mode and H-mode plasmas in the DIII-D tokamak to see if it corresponds with the stiffness picture under a variety of conditions, including strong localized heating with electron cyclotron waves (ECH) and variation of the plasma rotation (correlated to $E_r x B$ shear, which is expected to influence the stability of electrostatic turbulence) with changes in the applied torque through neutral beam injection (NBI).

The turbulence picture described above implies there should be a lack of variation in the temperature profiles. However, the converse is not true — the lack of variation in the profiles

cannot be used to infer uniquely the existence of the turbulent picture of stiffness. This can be seen by integrating the energy balance equation for a cylinder of length $2\pi R$ under the assumptions of stationary conditions, central heating, and a constant thermal conductivity κ to get the temperature scale length (a typical measure used to characterize the profile shape):

$$L_T \equiv aT(\rho)/|dT/d\rho| = [4\pi^2 R\kappa T(a)/P - ln(\rho)]a\rho \quad , \qquad (1)$$

where T is the temperature (in energy units here), a is the radius of the cylinder, P is the heating power, and ρ is the radius normalized to a. These approximations are likely too simplistic to use for data analysis, but point to the fundamental contributions that determine the temperature scale length. If the first term is negligible, the temperature scale length reduces to a simple geometric factor. Without the approximation of constant κ, this term will have a weak dependence on κ appearing as the ratio of the local value to the weighted integral of κ over the exterior part of the plasma. If the second term is negligible, the scale length also will vary only weakly in a power scan, as can be seen by the following argument. If the global confinement degrades with increasing P, then κ will increase with P. If the temperature at the top of the H mode pedestal also increases with P, consistent with experimental observations [7] including the data discussed here, then the first term is nearly constant. Also, the notion that the boundary temperature affects the internal profile shape is true without invoking the stiffness picture. Therefore, invoking a correlation of core and edge temperatures as a signature of the stiffness model is not valid. In the case of a model where the thermal conductivity has an explicit dependence on temperature, the integration becomes much more complicated [8]. This simple exercise motivates looking directly at the flux-gradient relationship in the experiment rather than the profile variations to test the hypothesis of stiffness. Ultimately, a validated model for the threshold and the transport due to turbulence is needed, if this picture holds true. Progress in model validation using the data presented here is reported separately [9].

The experiments reported here are of two types. In the first experiment, L-mode plasmas are heated by ECH locally at two locations ($\rho \approx 0.5$ and $\rho \approx 0.7$), with the amount at each location varied in increments of about 20% of the total power, holding the total power fixed. This scheme has the effect of keeping the power flow outside the outer heating point fixed (and thereby the temperature boundary condition fixed) while changing the power flow substantially at $\rho \approx 0.6$. This variation probes strongly the flux-gradient relationship at that point in the plasma. In the second experiment, the NBI heating power was scanned in H-mode plasmas for two different levels of torque input (controlled by the ratio of NBI in the co-current and counter-current directions). The plasma rotation driven by the injected torque is related to the radial electric field E_r. This variation probes strongly the influence of equilibrium E_rxB shear, which is believed to affect the level of turbulence in the plasma and therefore the transport significantly.

Two measures of stiffness will be used here. Ideally, one would define the stiffness S as the ratio of $\partial q/\partial|\nabla T|$ to $q/|\nabla T|$, which is the ratio of the incremental thermal conductivity to the equilibrium thermal conductivity. Here q is the energy flux conducted through a flux surface. The difficulty is that the partial derivative formally assumes that all other relevant quantities are held strictly fixed. This is not possible in experiments. As a proxy for this quantity, the ratio of the measured incremental thermal conductivity $\delta q/\delta|\nabla T|$ to the measured power

balance thermal conductivity $q/|\nabla T|$ will be used. The reader should keep in mind that variables relevant to transport other than the temperature gradient might not be constant. When available, the ratio of the incremental transport from heat pulse analysis to the power balance value will be used as a proxy for the ideal stiffness parameter. Again, there are significant issues with identifying the conductivities from heat pulse measurements with the "real" incremental transport, but it remains a useful qualitative measure.

2. L-Mode Plasmas

The plasma configuration for the L-mode experiment had an upper single null with ∇B down to avoid transition to H mode (Fig. 1). In addition, the plasma was limited on the centerpost to further inhibit H-mode transitions. Also shown in Fig. 1 is a schematic of the heating configuration used in these experiments. Six gyrotrons were used; the spatial distribution was varied from five gyrotrons aimed at the innermost point (ρ≈0.5) and 1 modulated gyrotron at the outer point (ρ≈0.7) to all the gyrotrons at the outer point. The average power delivered to the plasma from each gyrotron was about 500 kW and all ratios of inner to outer power were used except four inner and two outer. The ray path for the inner case stops at the second harmonic resonance because the power is calculated to be fully absorbed there. At the outer location, >94% of the power is calculated to be absorbed for the case shown, so the ray tracing continues until the ray reaches the plasma boundary. The carbon ion temperature, toroidal velocity, and density are taken from short pulses of NBI at the end of the analysis time; the pulse is assumed to be non-perturbative on this short time scale. Preliminary analysis of these plasmas has been published [10]; however, several diagnostic issues requiring reanalysis were encountered in the preparation of this work, some of which still need to be addressed. The conclusions of [10] remain qualitatively correct, but the specific values of some quantities may be somewhat different.

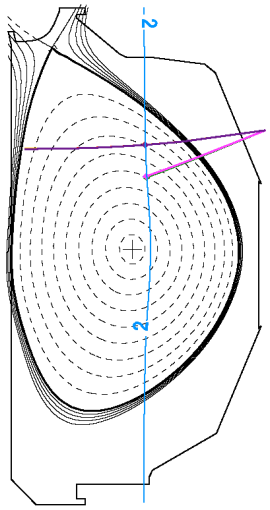

FIG. 1. Cross-section view of DIII-D plasmas used for the L-mode experiments. The blue vertical line is the location of the second harmonic cyclotron resonance for 110 GHz waves. The two lines show the calculated trajectories of EC waves aimed at ρ=0.5 and ρ=0.7.

The experimental design was intended to mimic as nearly as possible the typical flux-tube gyro-kinetic transport calculation where all quantities, except one, in this case the temperature gradient, are held fixed. The electron temperature profiles from ten plasmas comprising five separate heating variations are shown in Fig. 2. Since the total power is nearly constant, the temperature outside the outer ECH location (averaged over the modulation period of the EC power) is nearly constant. Between the two ECH locations (shown for the case with three gyrotrons aimed at each location), the temperature gradient varies by over nearly a factor of 4, while the temperature at r≈0.6 varies only by a factor of 1.4.

The resulting flux-gradient relationship for each of the ten L-mode plasmas is shown in Fig. 3. The flux is the power conducted through the surface at ρ≈0.6 in the electron channel from a standard power balance calculation. The thermal conductivity κ is the slope of a line connecting any data point in Fig. 3(a) with the origin. In Fig. 3(b), the flux normalized to the density and temperature scalings expected for gyroBohm transport and the gradient normalized to R/T are shown using R=1.7 m as the typical value of the major radius of the flux surface. The lack of substantive change with these normalizations is largely due to the experimental design, which minimized variation in the normalizations. It is clear from Fig. 3 that κ increases strongly for only a small increase in ∇T for the cases with three and five gyrotrons at the inner location. This is quantified in Fig. 4 where the two measures of stiffness are shown. The heat pulse analysis has been carried out allowing for the possibility of a convective term and a damping term in addition to the diffusion. Analysis of the heat pulses only considering diffusion would result in higher values for S. The power balance conductivity can be corrected for thermal convection using the heat pulse data, but that has not been done here. (Energy flux from particle convection has been excluded.)

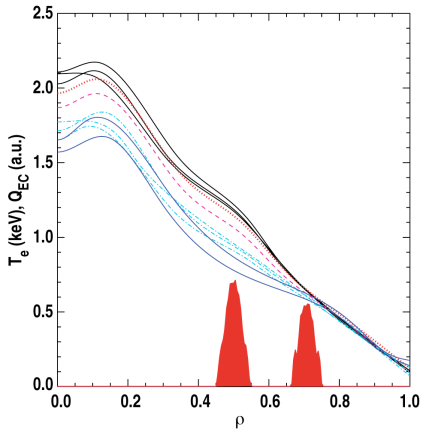

FIG. 2. Fitted electron temperature profiles from EC emission measurements for zero (blue solid lines), one (cyan dot-dashed lines), two (magenta dashed line), three (red dotted line), and five gyrotrons (black solid lines) at the inner heating location vs normalized radius. The two peaks indicate the radial locations of the inner and the outer heating. The ECH power density is shown for the case with three gyrotrons at the inner location and three (one modulated) at the outer location.

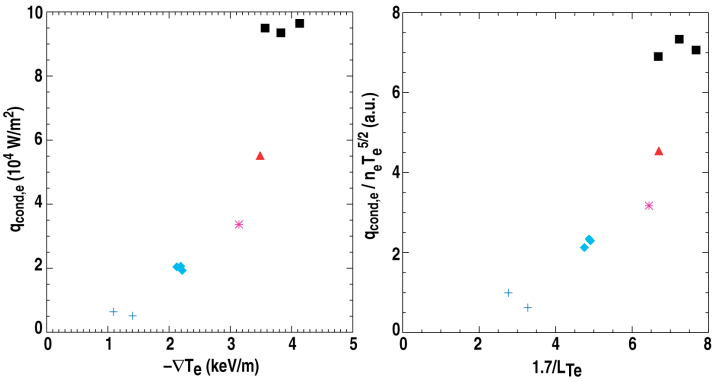

FIG. 3. (a) The conducted power in the electron channel from power balance analysis vs the measured electron temperature gradient. (b) The same data, but the flux normalized to the gyro-Bohm scaling and the gradient normalized to give R/L_{Te}. The various symbol colors correspond to the cases described in the caption of Fig. 2.

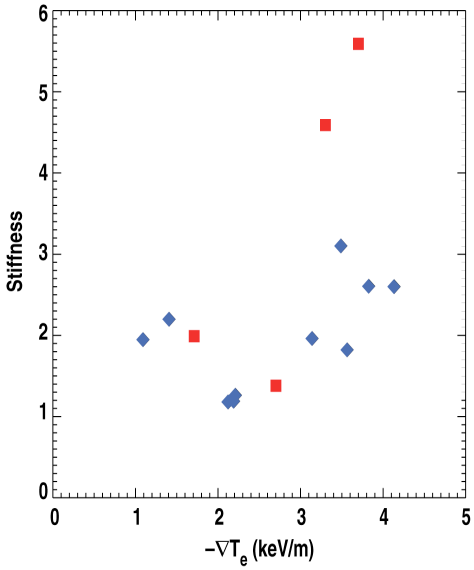

FIG. 4. Two proxies for the stiffness parameter vs. electron temperature gradient as defined in the text. The red squares are the incremental power thermal conductivity from finite difference of the power balance data. The blue diamonds are the ratio of the conductivity from heat pulse analysis to those from power balance analysis.

The heat pulse conductivity rises to about 3 times the power balance value for the highest gradients. The incremental conductivity derived from the power balance increases even more strongly with ∇T. An analysis of the uncertainties in both the gradient and flux have not been carried out; however, it seems unlikely that the qualitative feature of flux increasing more rapidly than the expected driving gradient shown in Figs 3 and 4 will be altered in any significant way. It appears that it only takes about 1 MW of power conducted to ρ=0.6 to give rise to a large increase in flux without a significant corresponding increase in the electron temperature gradient that is the expected source of free energy to drive the turbulence. This appears to correspond to the picture attributing the lack of profile variation to the onset of transport beyond a threshold gradient (here about 3 keV/m). The evidence of convective transport from the heat pulse analysis complicates the picture somewhat, and may explain some of the apparent strong increase in flux. The only other obvious possibility is that other parameters, such as parallel flows or gradients in other quantities are changing significantly, but a candidate quantity has not yet been identified from the data.

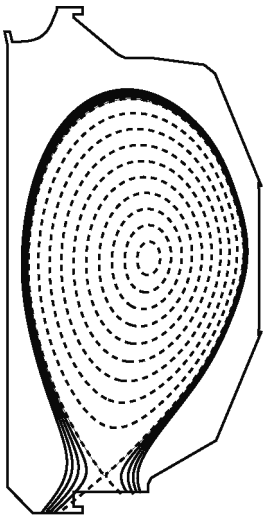

FIG. 5. Cross-section view of DIII-D plasmas used for the H-mode experiments.

3. H-mode Plasmas

For the H-mode experiments, a lower single-null plasma was chosen with ∇B down to lower the L-H transition power threshold. The plasma was designed to have weak shaping (Fig. 5) under the premise that this would minimize the variation in the edge boundary condition and reduce the sensitivity of the resulting changes in profile shape on the boundary conditions. The total NBI power was scanned from ~3–7 MW at a low value of applied torque (~1.5 Nm) and from ~3–9 MW at higher values of applied torque (~3–7 Nm). The low torque cases were achieved by injecting the proper ratio of co-current and counter-current NBI while the higher torque cases used all co-current NBI. The resulting ion and electron temperature profiles are shown in Fig. 6. The focus here will be on the ion transport.

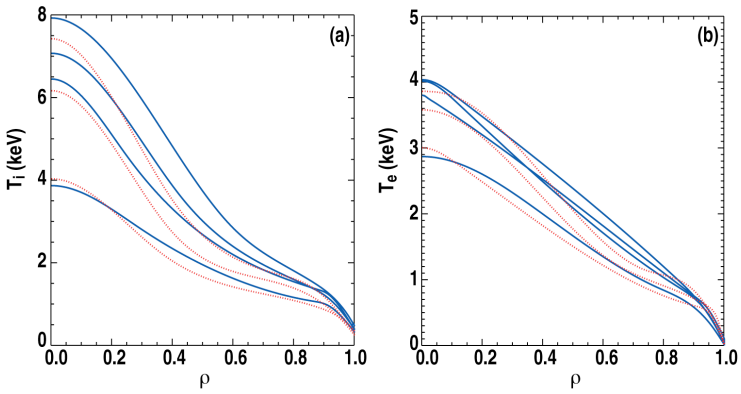

FIG. 6. (a) The fitted a) ion and b) electron temperatures vs. normalized radius. The solid blue lines are the high torque cases with roughly 3, 5, 7, and 9 MW of total applied power (bottom to top). The red dotted lines are the low torque cases with roughly 3, 5, and 7 MW of total applied power (bottom to top).

The flux-gradient relationship for the ions is shown for seven plasmas (three low torque, four high torque) at four different radii in Fig. 7. The solid lines in each of the panels is a linear fit to the two datasets (low and high torque) with each point equally weighted and without constraining the fit to pass through the origin. This allows an assessment of the stiffness proxy directly. If the fit passes through the origin, then S=1 and there is no stiffness. If the intercept at zero gradient is positive, as it is in

most cases, then the incremental transport is actually weaker than the average value. Only in the case that the intercept is negative would stiffness be indicated. The fact that the intercept is near zero or positive in virtually all cases shown in Fig. 7 implies the data does not support a picture where the gradients are fixed by very strong transport above a threshold value. The only case where such a picture may hold is the low torque case at ρ=0.7. In general, the transport is higher at low torque for the same gradient. If the E_rxB shear is correlated with the torque input as expected, the higher transport at low torque would be consistent with reduction in the underlying turbulence by E_rxB shear.

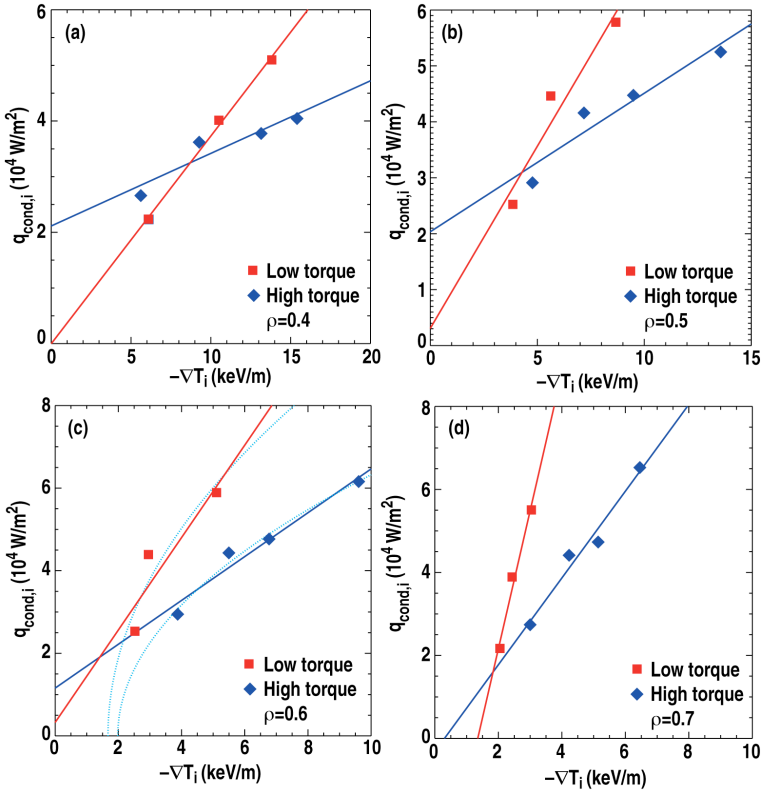

FIG. 7. The conducted power in the ion channel from power balance analysis vs. the measured ion temperature gradient for (a) ρ=0.4, (b) ρ=0.5, (c) ρ=0.6, and (d) ρ=0.7. The red squares are the low torque data and the blue diamonds are the high torque data. The significance of the lines is explained in the text.

On the question of a threshold, the data can be reconciled with a threshold as shown in Fig. 7(c) by fitting to a parabola opening to the right. The resulting fits show that both the low and high torque data can be reconciled with a common threshold gradient value (~1.5–2.0 keV/m) and stronger transport in the low torque case, consistent with weaker E_rxB shear. The picture of a common threshold and stronger transport at low torque is consistent with the data at all four radii shown. However, the data do not compel one to this explanation; the main evidence is the relative position of the data points at the lowest two power levels. An uncertainty analysis will be carried out to determine the confidence in the location of these points. But the fundamental issue with drawing a strong conclusion about a potential threshold is that the indicated threshold value lies below the range of the present data and is

likely unachievable under these plasma conditions since the fluxes near threshold are likely lower than those needed to operate in H mode.

The normalized fluxes and gradients for ρ=0.6 are shown in Fig. 8. The variation in both quantities is substantially smaller than the corresponding unnormalized quantities [Fig. 7(c)]. The fact that the flux variation is reduced implies the variation is described well by the expected gyro-Bohm scaling of the flux and the influence of other uncontrolled parameters is either weak or cancels out. The variation in the normalized gradient (R/L_{Ti}) is significant, which is inconsistent with the picture of strong transport above a threshold that is constant in temperature gradient scale length, but consistent with the lack of stiffness seen in the unnormalized data shown in Fig. 7.

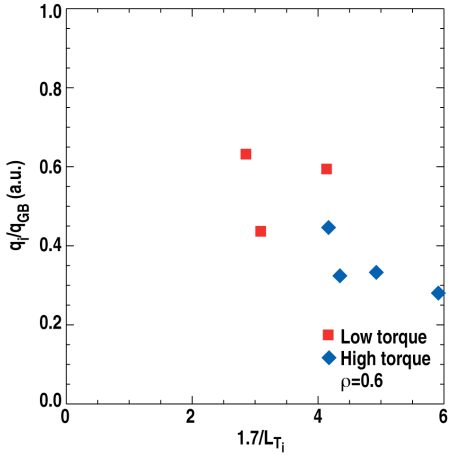

FIG. 8. The same data as Fig. 7(c) with the flux normalized to the gyro-Bohm scaling and the gradient normalized to give R/L_{Ti}.

4. Discussion

Two types of experiments were carried out to test the hypothesis that the lack of observed variation in temperature profiles is due to the onset of strong transport above a threshold gradient condition. In the first, highly localized ECH was applied at nearby radial locations to isolate the variation of the electron temperature gradient on the transport. Clear evidence supporting both a threshold gradient and the onset of strong transport without corresponding increase in gradient was presented. However, the power required to exceed this gradient is about 1 MW — a level exceeded in almost any auxiliary heated discharge in DIII-D. Therefore, the main utility of this study would appear to be testing of physics-based models to see that they capture the behavior in this regime, even though these models will likely be applied under conditions far from threshold. Although not shown here, similar tests with both co-current, balanced, and counter-current NBI in addition to the local ECH were made. Careful comparison of this data with models will provide a better test of their validity for predicting transport in more typical conditions farther from threshold.

The second type of experiment explored the same hypothesis of threshold plus strong transport in the H-mode regime at two values of applied torque. For the ion heat transport, no evidence was found for strong transport limiting the variation of the ion temperature gradient with additional heating power at low or high torque. The possible exception to this statement

was the case with low torque at ρ=0.7, which showed little variation in the ion temperature gradient despite an increase in heating power greater than a factor of 2. Circumstantial evidence for a common threshold in ion temperature gradient between the low and high torque cases was presented, but direct evidence is lacking because the value of this threshold is at or below that for sustaining the H-mode pedestal. The strength of this circumstantial evidence will be clearer following a proper uncertainty analysis. The motivation for an accurate prediction of the critical gradient may be reduced, given the lack of evidence for strong transport restricting the resulting gradients to be close to this value. Although not shown here, the electron heat transport in these plasmas is more consistent with the hypothesis of strong transport beyond a critical gradient and warrants further investigation.

This work was supported by the US Department of Energy under DE-FC02-04ER54698, DE-FG02-07ER54917, DE-FG02-94ER54235, DE-FG03-97ER54415, and DE-FG02-0854984. The authors acknowledge discussions with P. Mantica in the planning and analysis of the experiments.

References

[1] COPPI, B., Comments Plasma Phys. Controlled Fusion **5** (1980) 261
[2] DNESTROVSKY, Yu.N, et al., Plasma Physics Reports **28** (2002) 887
[3] COPPI, B. and PEGORARO, F., Phys. Fluids B **3** (1991) 2582
[4] HAMEIRI, E. and BHATTACHARJEE, A. Phys. Rev. A **35** (1987) 768
[5] LUCE, T.C., et al., Phys. Rev. Lett. **68** (1992) 52
[6] GARBET, X., et al., Plasma Phys. Control. Fusion **46** (2004) 1351
[7] MAGGI, C.F., et al., Nucl. Fusion **47** (2007) 535
[8] IMBEAUX, F. and GARBET, X., Plasma Phys. Controlled Fusion **44** (2002) 1425
[9] HOLLAND, C., et al., this conference
[10] DeBOO, J.C., et al., Phys. Plasmas **19** (2012) 082518